Naringenin alleviates hepatic injury in zinc oxide nanoparticles exposed rats: Impact on oxido-inflammatory stress and apoptotic cell death

Dalia Ibrahim El-wafaey [a], Ola Elsayed Nafea [b,c]*, Eman Mohamed Faruk [d]

[a] Department of Anatomy and Embryology, Faculty of Medicine, Zagazig University, Zagazig, Egypt

[b] Department of Forensic Medicine and Clinical Toxicology, Faculty of Medicine, Zagazig University, Zagazig, Egypt

[c] Department of Clinical Pharmacy, College of Pharmacy, Taif University, Taif, Saudi Arabia

[d] Department of Histology and Cell Biology, Faculty of Medicine, Benha University, Benha, Egypt

*Corresponding author:

Dr. Ola Elsayed Nafea

Department of Forensic Medicine and Clinical Toxicology

Faculty of Medicine

Zagazig University, Zagazig, Egypt

Zip code: 44519

Tel: +201026269962

E-Mail: olanafea@zu.edu.eg

oenafea@tu.edu.sa

Running title: NAR alleviates hepatic injury in ZnONPs exposed rats

Abstract

Human exposure to nanoparticles became unavoidable secondary to their massive involvement in a multitude of industrial applications. Zinc oxide nanoparticles (ZnONPs) are one of the most commonly used metal oxide nanoparticles in biological applications. Naringenin (NAR), a citrus-derived flavonoid, has favorable biological properties that promote human health. The present study was carried out to investigate the possible defensive role of NAR versus ZnONPs provoked hepatic injury in rats through an evaluation of liver enzymes, hepatic biomarkers of oxidative stress, inflammatory process, apoptotic cell death along with histopathological examination of liver tissue. Therefore, 32 adult rats were randomly divided into four equal groups as control, NAR, ZnONPs and co-treated ZnONPs with NAR groups. All treatments were administered for 14 days. Our results showed that ZnONPs induced hepatic injury as documented by the marked increased hepatic enzymes activities, disturbed hepatic oxidant/antioxidant balance, increased hepatic inflammatory reactions, in addition to, extensive hepatic morphological alterations, marked collagen fibers accumulation as well as overexpression of apoptotic BAX and the noticeable intensified positive nuclear staining for nuclear factor Kabba-b (NF-κB) in hepatic tissues. Concurrent NAR supplement to ZnONPs-treated rats significantly declined liver enzymes activities, restored oxidant/antioxidant balance, reversed inflammation, induced fewer collagen fibers accumulation, and antagonized BAX-mediated apoptotic cell death in hepatic tissues. We concluded that concurrent NAR supplement to ZnONPs treated rats improved hepatic function and structure by its antioxidant, anti-inflammatory and antiapoptotic potentials.

Keywords

Apoptosis; Hepatic injury; Naringenin; Nuclear factor Kabba-B; Zinc oxide nanoparticles

1. Introduction

Nowadays, a considerable interest in nanotechnology and its applications especially in medicine for diagnostic, therapeutic, and research purposes is appreciated. Nanotechnology can be defined as any procedure used to yield material in nano-scale structure with particle size varied from 1-100 nm (Ibrahim 2020). Human exposure to nanoparticles (NPs) became unavoidable in response to the massive involvement of nanotechnology in consumer products and industrial applications (Jeevanandam et al. 2018).

Zinc oxide nanoparticles (ZnONPs) are one of the most commonly used metal oxide nanoparticles (NPs) in biological applications secondary to their outstanding biocompatibility, cost-effectiveness, and less toxicity. In addition, ZnONPs have emerged as a promising technique in biomedicine, principally in the fields of imaging, anticancer, antimicrobial and antidiabetic therapies. In industrial fields, ZnONPs are utilized in various applications, such as coating, cosmetics, sunscreen, paint and, rubber industries (Jiang et al. 2018).

Human exposure to NPs occurs through natural activities. The environmental release of nanoparticulates, including; production, use, disposal, and waste treatment of nanoproducts-containing products, is the primary source for NPs exposure. The respiratory system and gastrointestinal tract are the most vulnerable boy systems to NPs health hazards owing to their nano-size and surface modifications. Inhalation is the primary route of NPs entry. Inhaled NPs can easily reach the circulation distributing into other sites in the human body involving the blood cells, heart, and liver (Buzea et al. 2007; Gnach et al. 2015). Previous experimental studies revealed the ability of NPs to induce toxicities in the various body organs. The liver is among these organ systems (Mansouri et al. 2015; Gupta and Xie 2018).

ZnONPs interfere with the activity and expression of hepatic cytochrome P450 (CYP450) enzymes and cause histological lesions in the liver. Moreover, zinc per se accumulates in the

liver and decreases the elimination of other drugs and chemicals, resulting in their accumulation and subsequent toxicities (Spaggiari et al. 2014; Tang et al. 2016).

Naringenin (NAR) is a citrus-derived flavonoid that belongs to the flavanones subclass. NAR is found in several fruits and vegetables, e.g., grapefruit, lemon, oranges, bergamot. NAR has favorable biological properties that promote human health. It has anti-inflammatory, antioxidant, antimicrobial, antiproliferative, immunomodulatory, pain-relieving, and anti-diabetogenic activities (Manchope et al. 2017; Salehi et al. 2019; Tutunchi et al. 2020). Earlier studies illuminated the valuable role of NAR against various human and animal models of liver injury, including, but limited to, alcohol, heavy metals, carbon tetrachloride (CCL4), hepatitis C virus, and nonalcoholic fatty liver disease (Hernández-Aquino and Muriel 2017; Gonçalves et al. 2017; Wang et al. 2020).

Accordingly, we implemented this work to investigate the possible defensive role of NAR versus ZnONPs provoked hepatic injury in rats through an evaluation of liver enzymes, hepatic biomarkers of oxidative stress, inflammatory process, apoptotic cell death along with the histopathological examination of liver tissue.

2. Materials and methods

Chemicals

We purchase ZnONPs (particle size <50 nm and CAS Number 677450) and NAR (CAS number N5893) from Sigma Aldrich, *St*. Louis, USA.

Characterization of ZnONPs

The transmission electron microscope (TEM) was used to characterize the shape and size of ZnONPs. The dispersion of ZnONPs was dropped on carbon-coated copper grid and dried at room temperature to examine via TEM. TEM measurements were performed at an accelerating

voltage of 80 kV (Model JEM-1400, JEOL Ltd., Tokyo, Japan). This characterization was conducted in Electron Microscopy Unit, Faculty of Agriculture Research Park (FARP), Cairo University, Eygpt.

Experimental protocol

Animal grouping and treatment

The study included 32 adult male albino rats aged 7-8 weeks and weighing 210-220 g. We purchased animals from the Zagazig Scientific and Medical Research Center (ZSMR) and maintained at the Breeding Animal House of Faculty of Medicine, Zagazig University, Zagazig, Egypt. All animals received humane care in compliance with the Animal Care Guidelines of the National Institutes of Health (NIH) and the Research Ethics Committee of Zagazig University approved the design of the study (ZU-IACUC/3/F/102/2020). For acclimation, the rats were handled manually before the experiment to allow biological stabilization for two weeks. The animals were housed in clean stainless-steel cages under standardized environmental conditions (temperature, 23±2 ℃, 12 h light/dark cycles, and humidity 60±5%) with free access to food and water.

Rats were weighed and randomly distributed into 4 groups (n =8):

Group I (Control): received 1 mL deionized water.

Group II (NAR): supplemented with NAR in a dose of 53 mg Kg^{-1} body weight (dissolved in 1 mL normal saline).

Group III (ZnONPs): treated with ZnONPs in a dose of 300 mg Kg^{-1} body weight, ZnONPs powder was dissolved in 1mL deionized water and was dispersed by ultrasonic vibration for 15 min.

Group IV (ZnONPs+NAR): supplemented with NAR in the same manner as in group II then rats treated with ZnONPs as in group III.

All treatments were given orally, once daily for consecutive 14 days.

The selection of the previous doses of NAR and ZnONPs was based on prior studies (Sharma, Singh, et al. 2012; Rebello et al. 2020). Dose conversion between different species was selected according to Reagan-Shaw et al. (2008).

Blood and hepatic homogenates preparation

Twenty-four hours after the last dose, we recorded animals' final body weights. Then rats were anesthetized with intraperitoneal (ip) injection of pentobarbital (60 mg Kg^{-1}) before blood samples collection (Leal Filho et al. 2005). Blood samples were collected from the retro-orbital venous plexus from each rat in the experimental groups into plain tubes, followed by centrifugation at 3000 rpm for 15 min for sera separation (stored at −20 °C) for assessment of liver enzymes. After that, animals were sacrificed by cervical dislocation, hepatic tissue specimens were dissected and then the homogenates were frozen rapidly at −80 °C for biochemical assays and histological examination.

Biochemical assays

Hepatic enzymes assessment

The serum activity for liver enzymes [alanine aminotransferase (ALT) and aspartate aminotransferase (AST)] was determined according to the proposed method of Reitman and Frankel (1957).

Hepatic antioxidant superoxide dismutase (SOD) enzyme activity and oxidative malondialdehyde (MDA) assessment

Both liver enzymatic activity of SOD and MDA level was colorimetrically assayed according to Nishikimi et al. (1972) and Ohkawa et al. (1979), respectively.

Hepatic proinflammatory/anti-inflammatory biomarkers [proinflammatory tumor necrosis factor-alpha (TNF-α) and anti-inflammatory interlukin-10 (IL-10)] assessment

Hepatic levels of TNF-α and IL-10 were assessed by the commercial ELISA kits (RayBiotech, USA, Cat No. ELH-TNFa-CL-1 for TNF-α, Cat No. ELH-IL10-CL-1 for IL-10) according to the manufacturer's recommendations.

Histological examination

The livers were dissected and fixed in 10% formal saline for processing of paraffin sections. Approximately 5-μm hepatic sections were cut and subjected to hematoxylin and eosin (Bancroft and Layton 2019a) and Mallory's trichrome (MT) stain (Bancroft and Layton 2019b).

Immunohistochemical study

Four μm, formalin-fixed, paraffin-embedded hepatic tissue sections were used for immunohistochemical examination (Sanderson et al. 2019). Hepatic tissue sections were deparaffinized in xylene and rehydrated in graded ethanol. Deparaffinized hepatic tissue sections were treated with hydrogen peroxide for 10 min to block non-specific peroxidase reactions. Microwave antigen retrieval was completed for 20 min in citrate buffer 0.01 M (pH 6.0). After washing with phosphate buffer saline, the slides were incubated for 60 min at room temperature with rabbit monoclonal antibodies; anti-Bax antibody (E63, 1:250, Abcam, UK) and anti-nuclear factor kappa-b (NF-κB) p65 antibody [E379] (ab32536). Visualization of the binding site of primary antibodies was made by the Dako EnVision™ kit (Dako, Copenhagen, Denmark). While visualization of the peroxidase reaction was done by incubating the hepatic sections with

diaminobenzidine (DAB) for 15 min. Mayer's hematoxylin was used for counterstaining the hepatic sections.

Histomorphometry assessment

Histomorphometry analysis of hepatic sections stained with MT, Bax and NF-κB was performed by Leica Qwin 500 Image Analyzer Computer System at Pathology Department, Faculty of Dentistry, Cairo University. Area percent of collagen fibers, Bax immunostaining, and percent of NF-κB positive nuclear immunostaining were assessed and measured five in non-overlapping histological fields /sections from each rat in the study groups.

Statistical analysis

Numerical variables are presented as the mean±standard deviation (SD). Shapiro-Wilk test (a test of normality) was used to check the normally distributed numerical variables. Bartlett's test was used to check the equality of variance. A one-way analysis of variance (ANOVA) or Welch's ANOVA test was performed according to equality of variance to detect statistical differences among groups. Post-hoc tests multiple comparisons tests were performed between groups (Bonferroni's test if equal variances were assumed; Dunnett's T3 test if equal variances were violated). Paired samples t- test was used to compare between final and initial body weights. The threshold of significance was $P < 0.05$. All statistical comparisons were two-tailed. All statistical calculations were conducted by Graphpad Prism, Version 8.0 Software (GraphPad Software, San Diego, CA, USA).

3. Results

Characterization of ZnONPs

TEM examination showed a well-dispersed ZnONPs. The shape was relatively spherical. The size ranged from 8.58 to 11.8 nm. (Fig. 1).

Mortality rates

We recorded no deaths in any of the study groups.

NAR supplement did not significantly change body weight in ZnONPs-treated rats

ZnONPs treatment for consecutive 14 days induced a statistically significant body weight loss compared with other groups of the study (P<0.05). Final body weight was similar to the initial weight in the NAR+ZnONPs group (213.8±8.8 vs 214.9±9.4, P=0.67). (Fig. 2).

NAR supplement declined the elevated liver enzymes induced by ZnONPs in rats

ZnONPs-intoxicated rats exhibited statistically significantly higher AST and ALT enzymes activities compared with other study groups (*P*<0.05). Concurrent NAR supplementation to ZnONPs-intoxicated rats induced a significant decline in AST and ALT enzymes activities (*P*=0.007 and *P*<0.001, respectively). (Table 1).

NAR supplement restored hepatic oxidant/antioxidant balance in ZnONPs-intoxicated rats

ZnONPs treatment caused a significant decline in hepatic SOD enzyme activity but a significant increase in hepatic MDA levels compared with control rats and NAR supplemented rats (*P*<0.001, each). Co-treatment with NAR produced a significant increase in hepatic SOD activity with a significant decrease in hepatic MDA levels compared with ZnONPs-intoxicated rats (*P*<0.001, each). (Table 1).

NAR supplement antagonized hepatic inflammatory reaction in ZnONPs-intoxicated rats

ZnONPs-intoxicated rats showed a statistically significant elevation in proinflammatory hepatic TNF-α concentration but a statistically significant decline in anti-inflammatory hepatic IL-10 concentration compared with control rats and NAR supplemented rats (*P*<0.001, each). Simultaneous NAR supplementation to ZnONPs-intoxicated rats significantly decreased

proinflammatory hepatic TNF-α concentration and significantly increased anti-inflammatory hepatic IL-10 concentration (P=0.049 and P=0.008, respectively). (Table 1).

Histological results

H&E-stained hepatic sections of the control and NAR-supplemented rats are similar and displayed the classical hepatic architecture where the liver cells were arranged in cords radiating from the central vein and separated by normal blood sinusoids. Normal portal areas are seen in the periphery of the hepatic lobules containing the portal veins, the bile ducts, and hepatic arteries (Fig. 3 a, b). Hepatic sections of ZnONPs-intoxicated rats showed a marked loss of the normal liver structure with distorted congested central veins and wide irregular sinusoids. Most of the hepatocytes are ballooned with deeply stained nuclei and vacuolated cytoplasm. The portal area showed a dilated congested portal vein with elongated endothelial lining and proliferation of bile duct, in addition to, some inflammatory cellular infiltration. Also, increased thickness of the muscular layer of the hepatic artery branches was seen in the portal area (Fig. 3c-e). Hepatic sections of the ZnONPs+NAR group showed variable degrees of hepatic architecture improvement in comparison to that of the ZnONPs group. Few hepatocytes showed deeply stained nuclei and less vacuolated cytoplasm. However, other hepatocytes had vesicular nuclei and acidophilic cytoplasm; some cells were binucleated. Slightly dilated congested blood sinusoids were seen. The portal area showed a marked reduction in cellular infiltration with a less dilated portal vein in comparison with the ZnONP group (Fig. 3f, g).

Mallory's trichrome -stained liver sections of control and NAR-supplemented rats were alike and showed a normal distribution of very few amounts of collagen fibers around the portal area (Fig. 4a). In the ZnONPs group, some blue-stained collagen fibers around the portal areas were evident (Fig. 4b). However, in the ZnONPs+NAR group, there was a marked reduction in

collagen fibers accumulation around the portal area compared to the ZnONPs group (Fig. 4c). Histomorophometry analysis of hepatic tissues showed that the mean area percent of hepatic collagen fibers disposition significantly increased in ZnONPs group compared with control rats and NAR supplemented rats ($P<0.001$, each). Concurrent NAR supplementation to ZnONPs-intoxicated rats significantly decreased the mean area percent of hepatic collagen fibers deposition compared with the ZnONPs group ($P=0.004$). (Fig. 4d).

Immunohistochemical results

Immunohistochemically stained sections with anti-Bax antibody control and NAR-supplemented rats showed a negative immune reaction for Bax inside the hepatocytes 'cytoplasm (Fig. 5a). While a strong positive reaction for Bax was detected in ZnONPs intoxicated rats (Fig. 5b). The reaction intensity was apparently diminished in ZnONPs+NAR group (Fig. 5c). Histomorophometry analysis of hepatic tissues showed that the mean area percent of Bax immunoexpression significantly increased in the ZnONPs group compared with control rats and NAR supplemented rats ($P<0.001$, each). While concurrent NAR supplementation to ZnONPs-intoxicated rats significantly decreased the mean area percent of hepatic Bax immunoexpression compared with ZnONPs group ($P<0.001$) (Fig. 5d).

Immunohistochemically stained sections with anti-NF-κB antibody of control and NAR-supplemented rats showing a negative immune reaction for NF-κB of hepatocytes nucleus (Fig. 6a). ZnONPs intoxicated rats showed a strong positive immune reaction for NF-κB of hepatocytes nucleus (Fig. 6b). While a weak positive immune reaction for NF-κB of the hepatocytes nucleus was observed in the ZnONPs+NAR group (Fig. 6c). Histomorophometry analysis showed that the positive nuclear staining for NF-κB significantly increased in the ZnONPs group compared with control rats and NAR supplemented rats ($P<0.001$, each). While

concurrent NAR supplementation to ZnONPs-intoxicated rats significantly decreased positive nuclear staining for NF-κB compared with ZnONPs group ($P<0.001$). (Fig. 6d).

4. Discussion

Previous in vivo and in vitro studies clarified the hepatotoxic effects of ZnONPs (Sharma et al. 2012; Sharma, Anderson, et al. 2012; Mansouri et al. 2015; Tang et al. 2016). Our findings showed that ZnONPs induced hepatic injury as documented by the marked increased hepatic enzymes activities, disturbed hepatic oxidant/antioxidant balance, increased hepatic inflammatory reactions, in addition to, extensive hepatic morphological alterations, marked collagen fibers accumulation as well as overexpression of apoptotic BAX and the noticeable intensified positive nuclear staining for NF-κB in hepatic tissues. These observed hepatic alterations are consistent with the former observations of Aboulhoda and coworkers (2020) who described similar biochemical, histopathological, and fibrotic changes in hepatic tissues of ZnONPs-exposed rats in a dose-dependent manner.

Bodyweight changes can be utilized as a critical indicator of the general health status of rats (Yousef et al. 2008). Weight loss can also signify the worsening of rats' general health conditions (Wang et al. 2021). Consequently, our findings showed that rats exposed to ZnONPs for 14 days significantly lost body weight. In corroboration, Ahmed et al. (2019) reported body weight loss in ZnONPs-treated rats.

Liver enzymes (ALT and AST) are the most sensitive indicators of the extent of hepatic injury and toxicity, especially ALT. These enzymes are cytoplasmic and are directly liberated into the circulation after cellular injury (Lin et al. 2000; Stockham and Scott 2008). In support, ZnONPs treatment caused a substantial increase in ALT and AST activities.

These findings are consistent with the findings of Mansouri et al. (2015) and Wang et al. (2008) who ascertained hepatic damage after oral exposure to ZnONPs in experimental animals. Conversely, a study of Surekha and coworkers (2012) reported non-significant alteration in ALT and AST enzymes activities after dermal exposure. This disagreement could be enlightened by the difference in the route of ZnONPs administration. In the present study, ZnONPs adversely influenced hepatic structures as manifested by the associated degenerative changes such as ballooning and cytoplasmic vacuolation of hepatocytes. These changes can be attributed to the ability of ZnONPs to elicit malfunction of hepatocytes' membranes with subsequent water and sodium inflow (Almansour et al. 2017).

We found that ZnONPs caused hepatic inflammation as evidenced by upregulation of the proinflammatory TNF-α, downregulation of anti-inflammatory IL-10, and overexpression of NF-κB in hepatic tissue along with scattered inflammatory cellular infiltrate in hepatic lobules and portal areas. Numerous prior experimental studies reported similar findings (Singh et al. 2020; Chen et al. 2021).

NF-κB is considered a pivotal inflammatory mediator that is involved in the initiation and progress of inflammatory processes. NF-κB can induce diverse proinflammatory genes expressions, such as genes-encoding for cytokines and chemokines expressions and contributes to inflammasome control. Therefore, NF-κB dysregulation can lead to the pathogenic processes of many inflammatory conditions (Guo et al. 2015; Liu et al. 2017). Specifically, NF-κB can stimulate the synthesis of a diversity of cytokines involved in acute and chronic hepatic inflammatory diseases (Muriel 2009; Fukui 2017; Maeda and Shibata 2017).

In the present work, ZnONPs exposure was associated with decreased activity of antioxidant SOD and increased levels of lipid peroxidation product MDA in hepatic tissue.

ZnONPs toxicity is linked to their solubility and ability to cause oxidative stress with the formation of free radicals. Free radicals negatively alter biomolecules functions such as nucleic acids, cellular enzymes, and biological membranes phospholipids (Yang et al. 2009; Osmond and Mccall 2010; Tang et al. 2016; Singh et al. 2020). The ability of ZnONPs to induce oxidative stress is linked to their ability to induce apoptotic cell death (Wang et al. 2014).

The current study revealed the defensive role of NAR against ZnONPs induced hepatic injury in rats. Concurrent NAR supplement to ZnONPs- treated rats showed a substantial improvement in hepatic function and structure. Prior studies reported the robust antioxidant and anti-inflammatory action of NAR (Alam et al. 2014). In a rat model of combination antiretroviral therapy (cART)-induced hepatotoxicity, Akang and coworkes (2020) displayed the anti-inflammatory potential of NAR by the downregulation of the proinflammatory TNF-α. In addition, Hernández-Aquino et al. (2019) attributed the anti-inflammatory potential of NAR in a rat model of CCL4 induced-hepatic toxicity to its ability to block NF-κB signaling pathway.

NAR has three phenolic groups and one keto group which can react with hydroxyl radicals, hydrogen peroxide and, peroxynitrite. Thus, NAR can inhibit oxidative stress harmful reactions. In addition, NAR diminished thiobarbituric acid reactive substances levels, lipid hydroperoxides. NAR can increase the enzymatic antioxidants activities in high cholesterol-fed rats (Jeon et al. 2007; Kannappan et al. 2010).

We found that NAR significantly decreased hepatic collagen fibers content. Consistently, Hua et al. (2021) pointed out the ability of NAR to reduce hepatic fibrosis in a mouse model of nonalcoholic steatohepatitis as documented by the decline in hepatic hydroxyproline content, a marker of collagen accumulation, transforming growth factor-β protein expression and α-smooth

muscle actin, the fundamental regulators of fibrosis, along with fewer MT-stained hepatic collagen fibers.

Our results showed that NAR can mitigate apoptotic changes triggered in the rat liver by ZnONPs treatment for 14 days, as evidenced by the downregulation of apoptotic Bax immunoexpression in hepatic tissues. In support, a study by Kannappan et al. (2010) concluded the antiapoptotic action of NAR in a high fructose diet receiving rats.

In conclusion, ZnONPs prompted hepatic injury in rats as shown by the manifest increased hepatic enzymes activities, hepatic oxidant/antioxidant imbalance, hepatic inflammatory reactions as well as extensive hepatic structural alterations, marked collagen fibers accumulation, overexpression of apoptotic BAX, and the obvious intensified positive nuclear staining for NF-κB in hepatic tissues. The current study underlined the defensive role of NAR against ZnONPs induced hepatic injury. Concurrent NAR administration to ZnONPs treated rats improved hepatic function and structure by its antioxidant, anti-inflammatory and, antiapoptotic potentials.

Funding. None.

Conflict of Interest

The authors report no declaration of competing interest.

References

-Aboulhoda BE, Abdeltawab DA, Rashed LA, Abd Alla MF, Yassa HD. 2020. Hepatotoxic effect of oral zinc oxide nanoparticles and the ameliorating role of selenium in rats: a histological, immunohistochemical and molecular study. Tissue Cell. 67:101441. DOI:10.1016/j.tice.2020.101441.

-Ahmed AFA, Ibrahim IA, El.mokhtar H, Morsy MM. 2019. Effect of zinc oxide

nanoparticles on the structure of testis of adult albino rats and the possible protective role of naringenin. Med J Cairo Univ. 87(September):3469-3483.

-Akang EN, Dosumu OO, Okoko IE, Faniyan O, Oremosu AA, Akanmu AS. 2020. Microscopic and biochemical changes on liver and kidney of Wistar rats on combination antiretroviral therapy: the impact of naringenin and quercetin. Toxicol Res (Camb). 9(5):601-608.

-Alam MA, Subhan N, Rahman MM, Uddin SJ, Reza HM, Sarker SD. 2014. Effect of citrus flavonoids, naringin and naringenin, on metabolic syndrome and their mechanisms of action. Adv Nutr. 5(4):404-417.

-**Almansour MI, Alferah MA, Shraideh ZA, Jarrar BM. 2017.** Zinc oxide nanoparticles hepatotoxicity: histological and histochemical study. Environ Toxicol Pharmacol. 51:124-130.

-Bancroft JD, Layton C. 2019a. The hematoxylin and eosin. In: Suvarna SK, Layton C, Bancroft JD, editors. Bancroft's theory and practice of histological techniques. 8th ed. Philadelphia (PA): Elsevier; p. 126-138.

-Bancroft JD, Layton C. 2019b. Connective tissue and other mesenchymal tissues with their stains. In: Suvarna SK, Layton C, Bancroft J, editors. Bancroft's theory and practice of histological techniques. 8th ed. Philadelphia (PA): Elsevier; p. 153-175.

-Buzea C, Pacheco II, Robbie K. 2007. Nanomaterials and nanoparticles: sources and toxicity. Biointerphases. 2(4):MR17-MR71.

-Chen L, Wu H, Hong W, Aguilar ZP, Fu F, Xu H. 2021. The effect of reproductive toxicity induced by ZnO NPs in mice during early pregnancy through mitochondrial apoptotic pathway. Environ Toxicol. 36(6):1143-1151.

-Fukui H. 2017. Cytokines in hepatic injury. In: Muriel P, editor. Liver pathophysiology:

therapies and antioxidants. 1st ed. Waltham: Elsevier; p. 341-354.

-Gnach A, Lipinski T, Bednarkiewicz A, Rybka J, Capobianco JA. 2015. Upconverting nanoparticles: assessing the toxicity. Chem Soc Rev. 44(6):1561-1584.

-Gonçalves D, Lima C, Ferreira P, Costa P, Costa A, Figueiredo W, Cesar T. 2017. Orange juice as dietary source of antioxidants for patients with hepatitis C under antiviral therapy. Food Nutr Res. 61(1):1296675. DOI: 10.1080/16546628.2017.1296675.

-Guo H, Callaway JB, Ting JP-Y. 2015. Inflammasomes: mechanism of action, role in disease, and therapeutics. Nat Med. 21(7):677-687.

-Gupta R, Xie H. 2018. Nanoparticles in daily life: applications, toxicity and regulations. J Environ Pathol Toxicol Oncol. 37(3):209-230.

-Hernández-Aquino E, Muriel P. 2017. Naringenin and the liver. In: Muriel P, editor. Liver pathophysiology: therapies and antioxidants. Waltham: Elsevier; p. 633-651.

-Hernández-Aquino E, Quezada-Ramírez MA, Silva-Olivares A, Casas-Grajales S, Ramos-Tovar E, Flores-Beltrán RE, Segovia J, Shibayama M, Muriel P. 2019. Naringenin attenuates the progression of liver fibrosis via inactivation of hepatic stellate cells and profibrogenic pathways. Eur J Pharmacol. 865:172730. DOI: 10.1016/j.ejphar.2019.172730.

-Hua YQ, Zeng Y, Xu J, Xu X L. 2021. Naringenin alleviates nonalcoholic steatohepatitis in middle-aged Apoe−/−mice: role of SIRT1. Phytomedicine. 81:153412. DOI:10.1016/j.phymed.2020.153412.

-Ibrahim H. 2020. Nanotechnology and its applications to medicine: an overview. QJM An Int J Med. 113(Supplement_1). DOI: 10.1093/qjmed/hcaa060.008/5829517

-Jeevanandam J, Barhoum A, Chan YS, Dufresne A, Danquah MK. 2018. Review on nanoparticles and nanostructured materials: history, sources, toxicity and regulations. Beilstein J

Nanotechnol. 9:1050-1074.

-**Jeon SM, Kim HK, Kim HJ, Do GM, Jeong TS, Park YB, Choi MS. 2007.** Hypocholesterolemic and antioxidative effects of naringenin and its two metabolites in high-cholesterol fed rats. Transl Res. 149(1):15-21.

-**Jiang J, Pi J, Cai J. 2018.** The advancing of zinc oxide nanoparticles for biomedical applications. Bioinorg Chem Appl. 2018:1-18. DOI: 10.1155/2018/1062562.

-**Kannappan S, Palanisamy N, Anuradha CV. 2010.** Suppression of hepatic oxidative events and regulation of eNOS expression in the liver by naringenin in fructose-administered rats. Eur J Pharmacol. 645(1-3):177-184.

-**Leal Filho MB, Morandin RC, Almeida AR de, Cambiucci EC, Metze K, Borges G, Gontijo JAR. 2005.** Hemodynamic parameters and neurogenic pulmonary edema following spinal cord injury: an experimental model. Arq Neuropsiquiatr. 63(4):990-996.

-**Lin SC, Chung TC, Lin CC, Ueng TH, Lin YH, Lin SY, Wang LY. 2000.** Hepatoprotective effects of *Arctium lappa* on carbon tetrachloride- and acetaminophen-induced liver damage. Am J Chin Med. 28(02):163-173.

-**Liu T, Zhang L, Joo D, Sun SC. 2017.** NF-κB signaling in inflammation. Signal Transduct Target Ther. 2:17023. DOI:10.1038/sigtrans.2017.23.

-**Maeda S, Shibata W. 2017.** Nuclear factor-kappa B actions during the development of hepatocellular carcinoma. In: Muriel P, editor. Liver pathophysiology: therapies and antioxidants. 1st ed. Waltham: Elsevier; p. 289-293.

-**Manchope MF, Casagrande R, Verri WA. 2017.** Naringenin: an analgesic and anti-inflammatory citrus flavanone. Oncotarget. 8(3):3766-3767.

-**Mansouri E, Khorsandi L, Orazizadeh M, Jozi Z. 2015.** Dose-dependent hepatotoxicity

effects of Zinc oxide nanoparticles. Nanomed J. 2(4):273-282.

-Muriel P. 2009. NF- κ B in liver diseases: a target for drug therapy. J Appl Toxicol. 29(2):91-100.

-Nishikimi M, Appaji N, Yagi K. 1972. The occurrence of superoxide anion in the reaction of reduced phenazine methosulfate and molecular oxygen. Biochem Biophys Res Commun. 46(2):849-854.

-Ohkawa H, Ohishi N, Yagi K. 1979. Assay for lipid peroxides in animal tissues by thiobarbituric acid reaction. Anal Biochem. 95(2):351-358.

-Osmond MJ, Mccall MJ. 2010. Zinc oxide nanoparticles in modern sunscreens: an analysis of potential exposure and hazard. Nanotoxicology. 4(1):15-41.

-Reagan-Shaw S, Nihal M, Ahmad N. 2008. Dose translation from animal to human studies revisited. FASEB J. 22(3):659-661.

-Rebello CJ, Beyl RA, Lertora JJL, Greenway FL, Ravussin E, Ribnicky DM, Poulev A, Kennedy BJ, Castro HF, Campagna SR, et al. 2020. Safety and pharmacokinetics of naringenin: a randomized, controlled, single-ascending-dose clinical trial. Diabetes Obes Metab. 22(1):91-98.

-Reitman S, Frankel S. 1957. A colorimetric method for the determination of serum glutamic oxalacetic and glutamic pyruvic transaminases. Am J Clin Pathol. 28(1):56-63.

-Salehi B, Fokou P, Sharifi-Rad M, Zucca P, Pezzani R, Martins N, Sharifi-Rad J. 2019. The therapeutic potential of naringenin: a review of clinical trials. Pharmaceuticals (Basel). 12(1):11. DOI: 10.3390/ph12010011.

-Sanderson T, Wild G, Cull AM, Marston J, Zardin G. 2019. Immunohistochemical and immunofluoresent techniques In: Suvarna SK, Layton C, Bancroft JD, editors. Bancroft's theory

and practice of histological techniques. 8th ed. Philadelphia (PA): Elsevier; p. 337-396.

-Sharma V, Anderson D, Dhawan A. 2012. Zinc oxide nanoparticles induce oxidative DNA damage and ROS-triggered mitochondria mediated apoptosis in human liver cells (HepG2). Apoptosis. 17(8):852-870.

-Sharma V, Singh P, Pandey AK, Dhawan A. 2012. Induction of oxidative stress, DNA damage and apoptosis in mouse liver after sub-acute oral exposure to zinc oxide nanoparticles. Mutat Res Toxicol Environ Mutagen. 745(1-2):84-91.

-Singh S, Gautam U, Manvi FV. 2020. Protective impact of edaravone against Zno NPs-induced oxidative stress in the human neuroblastoma SH-SY5Y cell line. Cell Mol Neurobiol. DOI: 10.1007/s10571-020-01011-0.

-Spaggiari D, Geiser L, Daali Y, Rudaz S. 2014. A cocktail approach for assessing the in vitro activity of human cytochrome P450s: an overview of current methodologies. J Pharm Biomed Anal. 101:221-237.

-Stockham SL, Scott MA. 2008. Liver function. In: Fundamentals of veterinary clinical pathology. 2nd ed. Hoboken: Wiley-Blackwell; p. 675-706.

-Surekha P, Kishore AS, Srinivas A, Selvam G, Goparaju A, Reddy PN, Murthy PB. 2012. Repeated dose dermal toxicity study of nano zinc oxide with Sprague-Dawley rats. Cutan Ocul Toxicol. 31(1):26-32.

-Tang HQ, Xu M, Rong Q, Jin RW, Liu QJ, Li YL. 2016. The effect of ZnO nanoparticles on liver function in rats. Int J Nanomedicine. 11:4275-4285.

-Tutunchi H, Naeini F, Ostadrahimi A, Hosseinzadeh-Attar MJ. 2020. Naringenin, a flavanone with antiviral and anti-inflammatory effects: a promising treatment strategy against COVID-19. Phyther Res. 34(12):3137-3147.

-**Wang B, Feng W, Wang M, Wang T, Gu Y, Zhu M, Ouyang H, Shi J, Zhang F, Zhao Y, et al. 2008.** Acute toxicological impact of nano- and submicro-scaled zinc oxide powder on healthy adult mice. J Nanoparticle Res. 10(2):263-276.

-Wang J, Deng X, Zhang F, Chen D, Ding W. 2014. ZnO nanoparticle-induced oxidative stress triggers apoptosis by activating JNK signaling pathway in cultured primary astrocytes. Nanoscale Res Lett. 9(1):117. DOI: 10.1186/1556-276X-9-117.

-Wang J, Zhu H, Lin S, Wang K, Wang H, Liu Z. 2021. Protective effect of naringenin against cadmium-induced testicular toxicity in male SD rats. J Inorg Biochem. 214:111310. DOI: 10.1016/j.jinorgbio.2020.111310.

-**Wang Q, Ou Y, Hu G, Wen C, Yue S, Chen C, Xu L, Xie J, Dai H, Xiao H, et al. 2020.** Naringenin attenuates non-alcoholic fatty liver disease by down-regulating the NLRP3/NF-κB pathway in mice. Br J Pharmacol. 177(8):1806-1821.

-Yang H, Liu C, Yang D, Zhang H, Xi Z. 2009. Comparative study of cytotoxicity, oxidative stress and genotoxicity induced by four typical nanomaterials: the role of particle size, shape and composition. J Appl Toxicol. 29(1):69-78.

-**Yousef MI, El-Demerdash FM, Radwan FME. 2008.** Sodium arsenite induced biochemical perturbations in rats: Ameliorating effect of curcumin. Food Chem Toxicol. 46(11):3506-3511.

Table 1. Effects of NAR on hepatic enzymes and hepatic biomarkers of oxidative stress, inflammation and apoptosis pathway in ZnONPs-induced hepatic injury in rats.

Parameter	Groups			
	Control	NAR	ZnONPs	NAR+ZnONPs
ALT (IU/L)	40.1±8.8†	40.24±5.6†	153.7±18.3‡	73.8±14.8§
AST (IU/L)	113.1±9.5†	121.9±3.5†	210.8±35.3‡	149.7±8.1§
SOD (U/g)	136.1±4.8†	140.7±6.7†	70.6±4.3‡	109.9±6.3§
MDA (nmol/g)	8.5±3.4†	7.3±1.6†	20.8±4.0‡	13.6±2.9§
TNF-α (pg/ 100 µg protein)	13.1±2.5†	12.2±2.6†	23.8±4.1‡	19.4±2.8§
IL-10 (pg/ 100 µg protein)	12.9±2.1†	13.4±1.5†	4.5±1.0‡	7.7±2.3§

All values are presented as mean±SD, n=8. means in a row without a common symbol significantly differ (P<0.05) by a one-way ANOVA followed by post hoc Bonferroni's multiple comparisons test or Welch's one-way ANOVA followed by post hoc Dunnett's T3 multiple comparisons test. Abbreviations; ALT, Alanine aminotransferase; AST, Alanine aminotransferase; SOD, Superoxide dismutase; MDA, Malondialdehyde; TNF-α, Tumor necrosis factor-alpha; IL-10, Interleukin-10; NAR, Naringenin; ZnONPs, Zinc oxide nanoparticles.

Figure legends

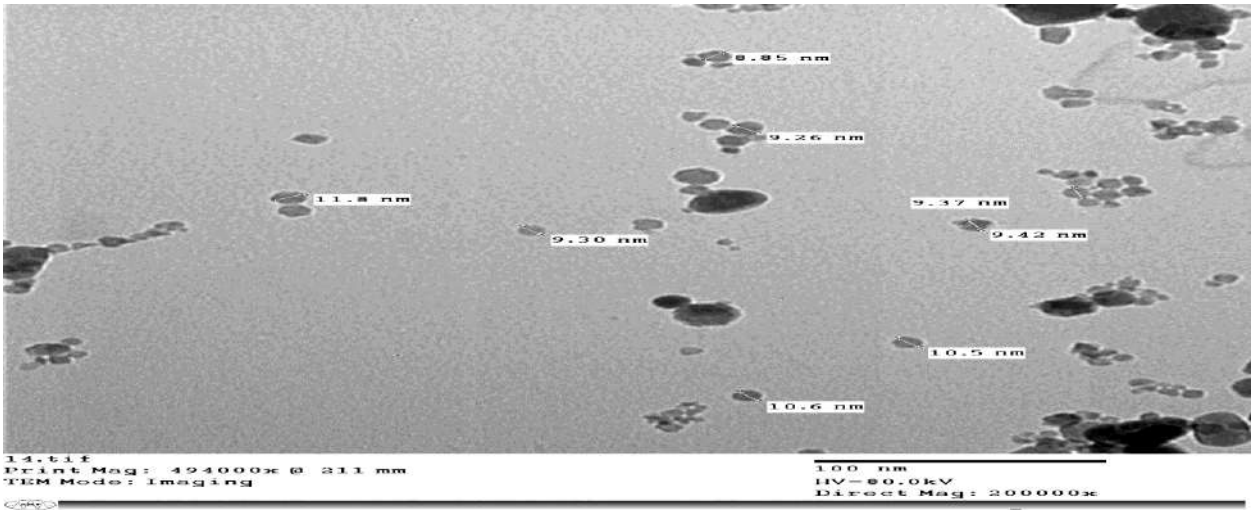

Fig. 1 Transmission electron microscopy image of zinc oxide nanoparticles

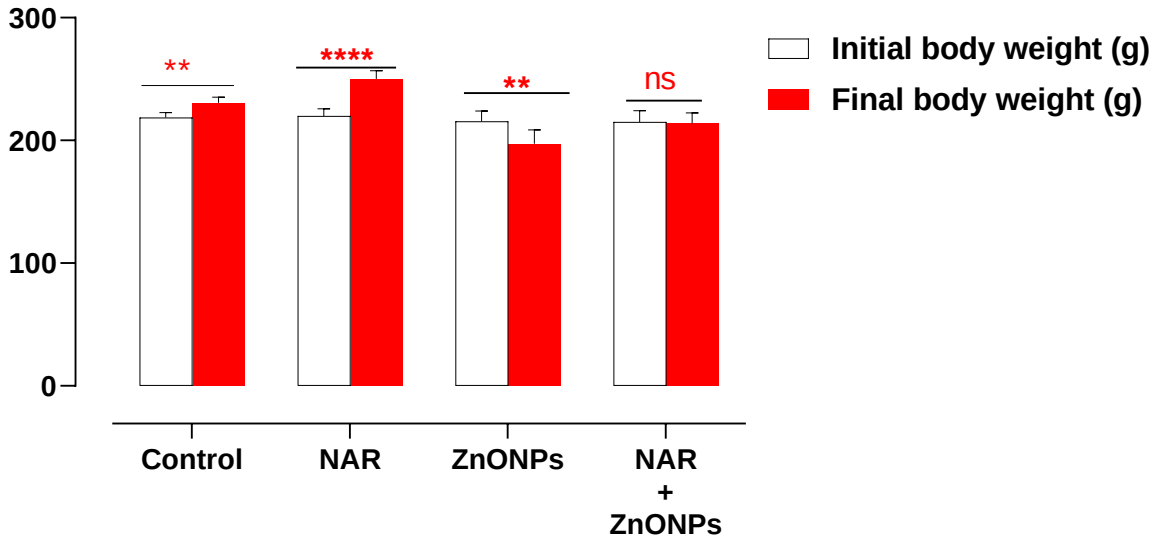

Fig. 2 Effects of NAR on body weight in in the rat ZnONPs-induced liver injury model. Comparison between final body weight vs initial body weight by paired samples t-test. ns, a non-significant difference, ** P <0.01, *** P <0.0001.

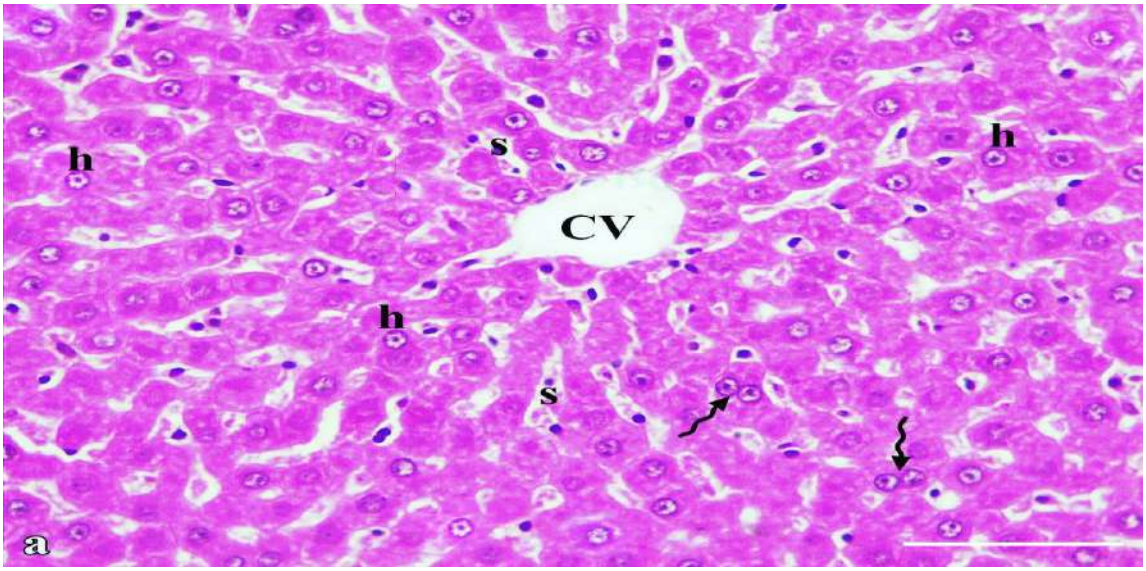

Fig. 3a: Control group showing central vein (CV) surrounded by radiating cords of polygonal hepatocytes. Hepatocytes (h) had rounded euchromatic vesicular nuclei and acidophilic cytoplasm. Blood sinusoids (s) are radiating with average size in between liver cords. Binucleated cell is also seen (zigzag arrow) in some cells. H&E × 400, scale bar, 50 μm

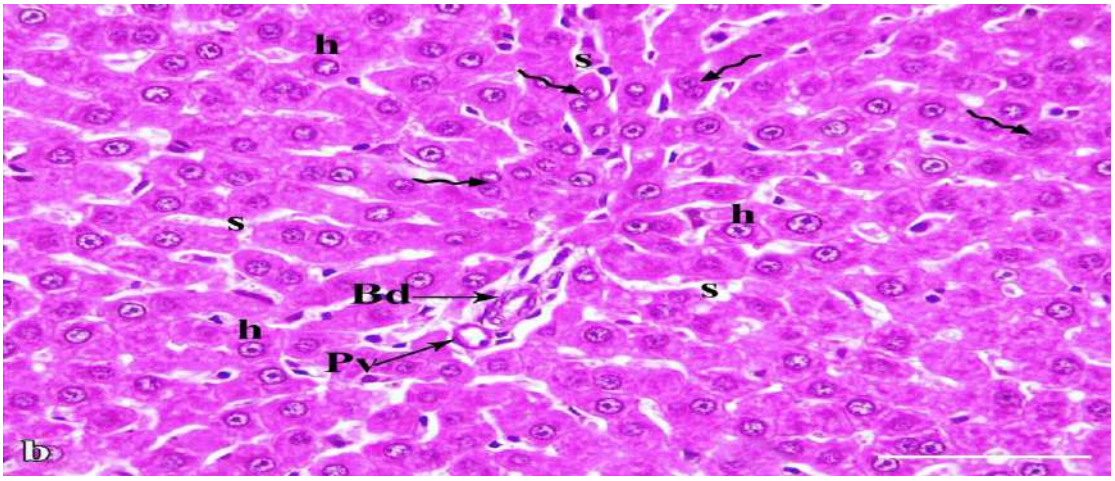

Fig. 3b: Control rats showing portal area containing portal vein (Pv) with a thin wall and bile duct (Bd). Polygonal hepatocytes (h) with rounded vesicular nuclei and acidophilic cytoplasm are seen. Notice, narrow radiating blood sinusoids (s) in between liver cords. Binucleated cells are also seen (zigzag arrows). H&E × 400, scale bar, 50 μm

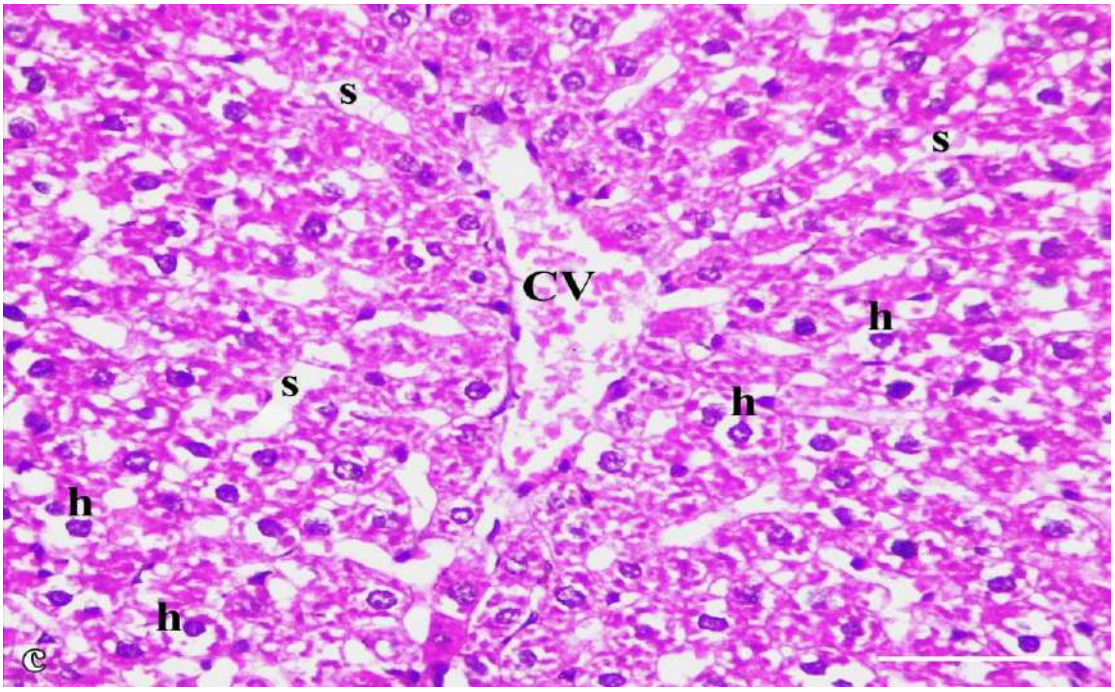

Fig. 3c: ZnONPs group showing a dilated distorted congested central vein (CV) with wide irregular sinusoids (S). Ballooning of hepatocytes (h) with darkly stained nuclei and vacuolated cytoplasm are observed. H&E × 400, scale bar, 50 μm

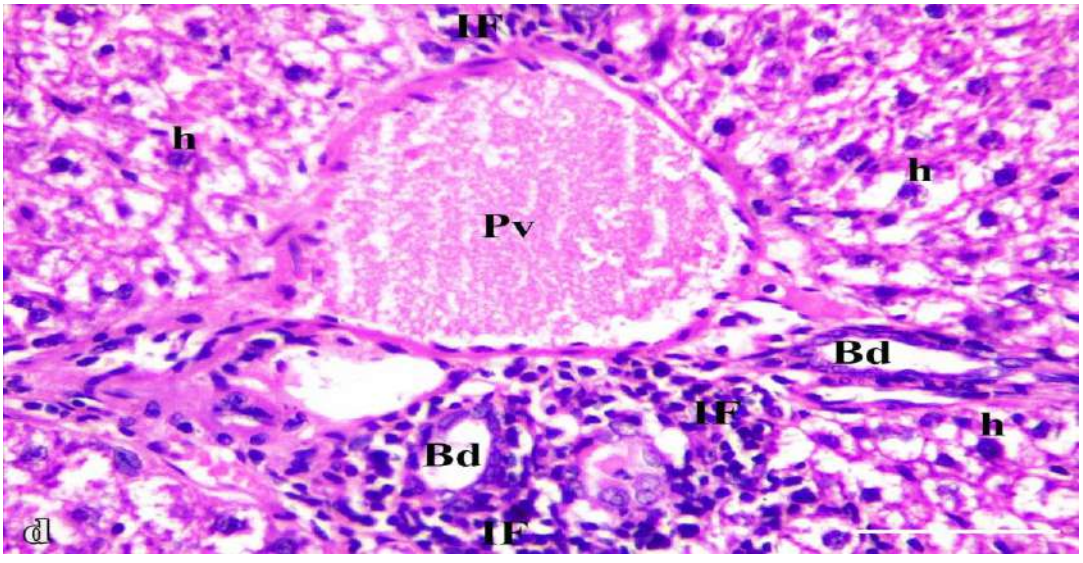

Fig. 3d: ZnONPs group showing a large, congested portal vein (Pv) with elongation of their endothelial lining and proliferation of bile duct (Bd). Mononuclear cellular infiltration (IF) in portal area and hepatocytes (h) with vacuolated cytoplasm and darkly stained nuclei. H&E × 400, scale bar, 50 μm.

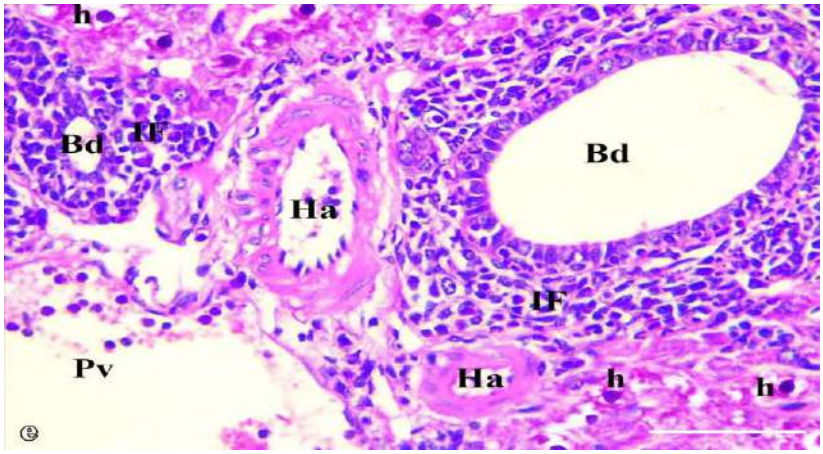

Fig. 3e: ZnONPs group showing proliferation of bile duct (Bd) and mononuclear cellular infiltration (IF) in the portal area. Hepatic artery (Ha) branch showed thickening in muscular layer and elongation of endothelial lining. Dilated Portal vein (Pv) and vacuolated hepatocytes (h) with dark nuclei are also observed. H&E × 400, scale bar, 50 μm.

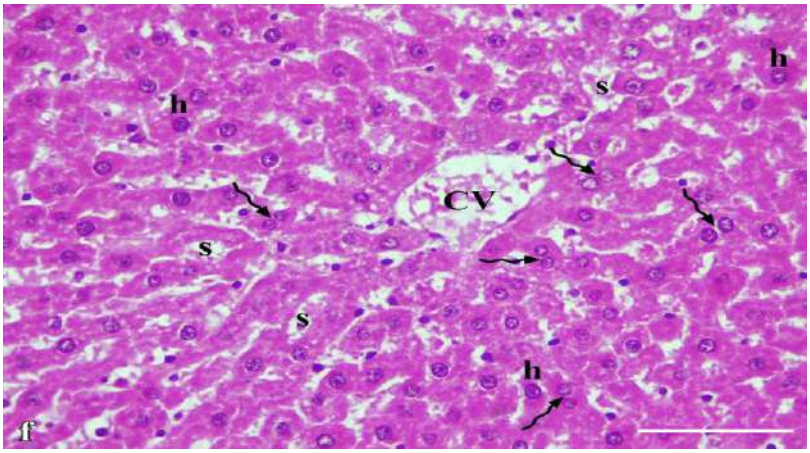

Fig. 3f: ZnONPs+NAR group showing slightly dilated congested sinusoids (S) and central vein (CV) with flat endothelial lining. Most of hepatocytes (h) had vesicular nuclei and acidophilic cytoplasm. Few cells showed darkly stained nuclei (h) and less vacuolated cytoplasm. Many binucleated cells (zigzag arrows) are also seen. H&E × 400, scale bar, 50 μm

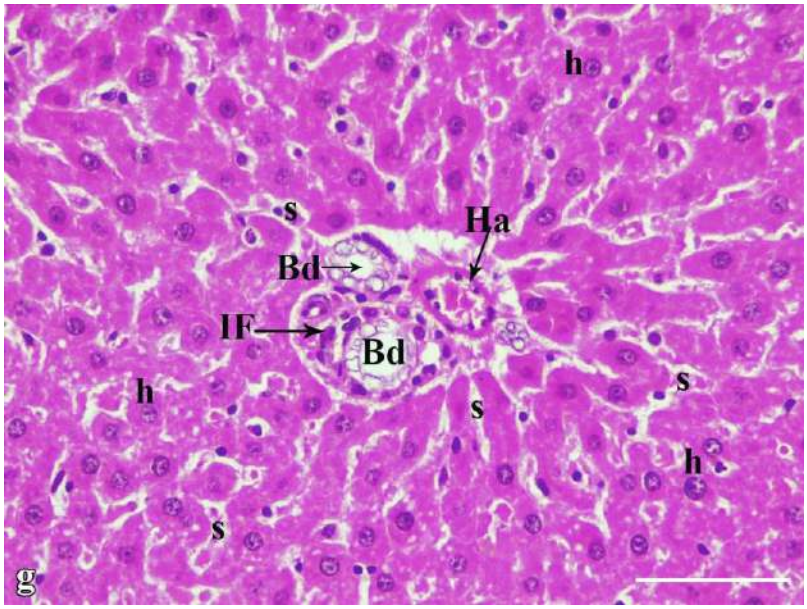

Fig. 3g. ZnONPs+NAR group showing portal area including hepatic artery (Ha), some degree of bile duct proliferation (Bd) and few mononuclear inflammatory cells (IF). Most of hepatocytes (h) had vesicular nuclei and acidophilic cytoplasm. Slightly dilated congested sinusoids (s) are also seen. H&E × 400, scale bar, 50 μm

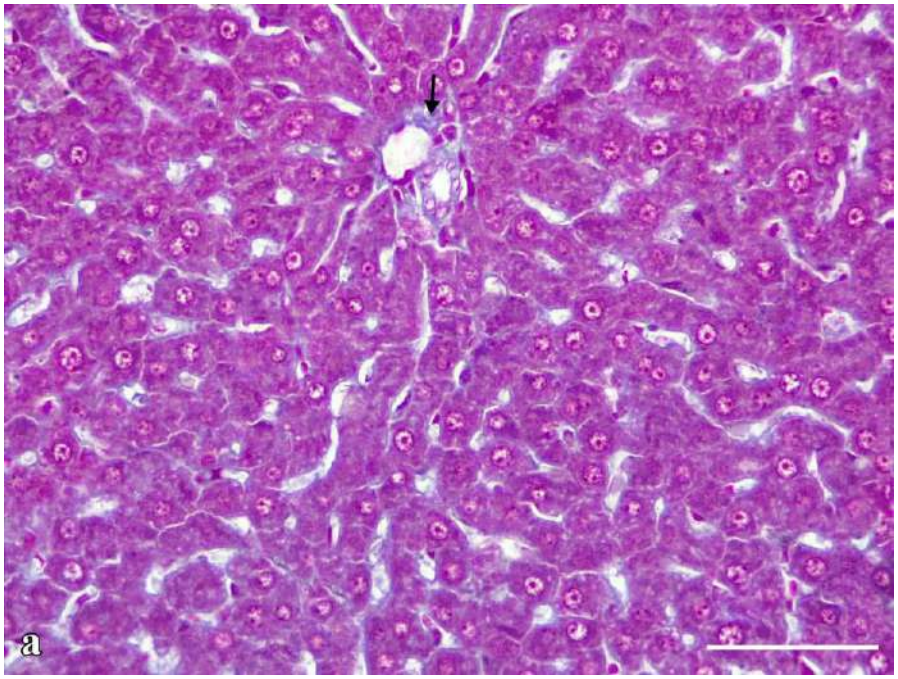

Fig. 4a Control group showing normally distributed collagen fibers (arrow). MT × 400, scale bar, 50 μm.

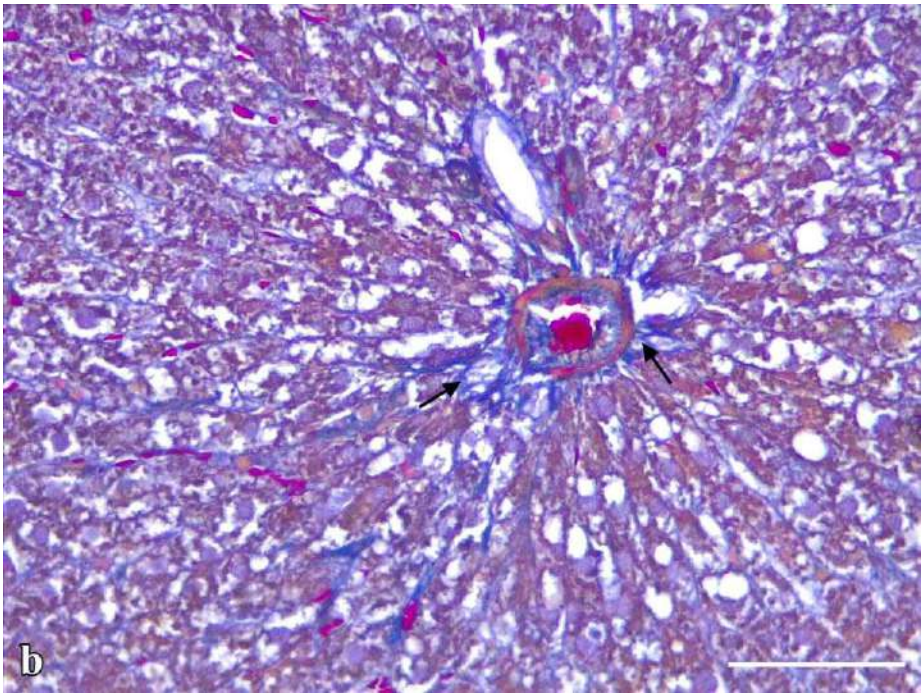

Fig. 4b ZnONPs group showing excess collagen fibers surrounding the portal area (arrows). MT × 400, scale bar, 50 μm.

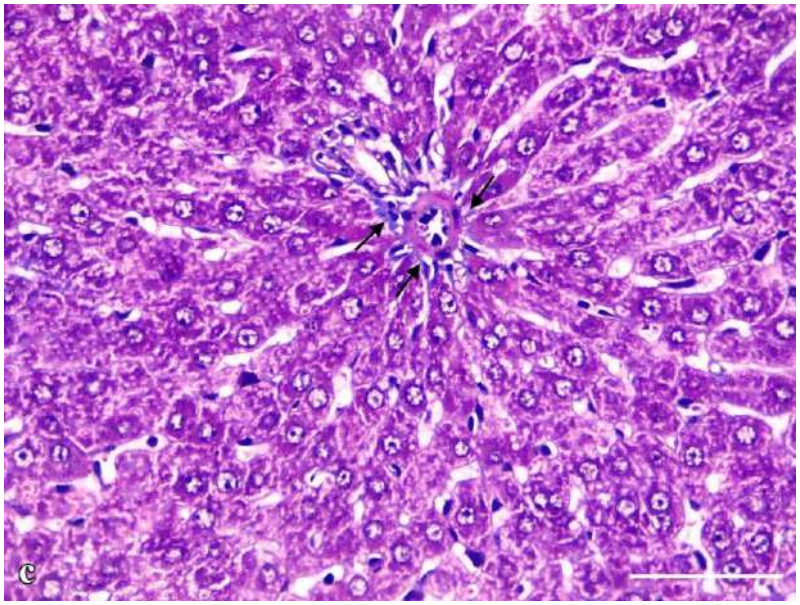

Fig. 4c ZnONPs+NAR group showing a reduction of the collagen content in portal area (arrows). MT × 400, scale bar, 50 μm.

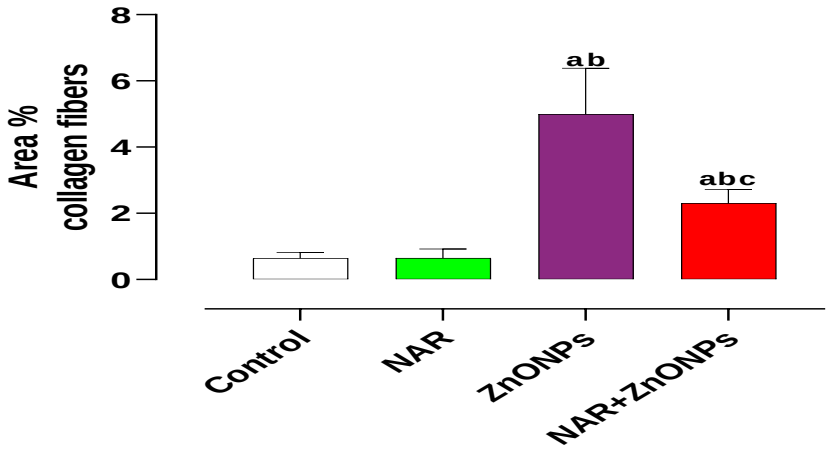

ig. 5d Effects of NAR on area percent collagen fibers deposition in the rat ZnONPs-induced liver injury model. Data are mean ± standard deviation, *n*= 8. [a] significant vs control group, [b] significant vs NAR group and [c] significant vs ZnONPs group by Welch's ANOVA test followed by Dunnett's T3 test post-hoc multiple comparisons tests, at a *P*-value < 0.05. Abbreviations; NAR, Naringenin; ZnONPs, Zinc oxide nanoparticles.

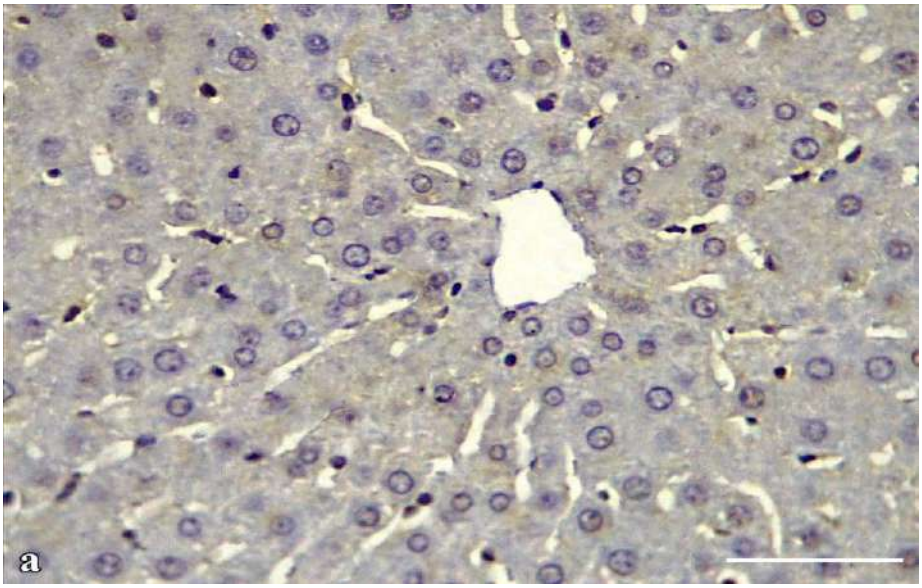

Fig. 5a Control group showing negative immune reaction for Bax inside the cytoplasm of hepatocytes (arrow). Bax × 400, scale bar, 50 μm.

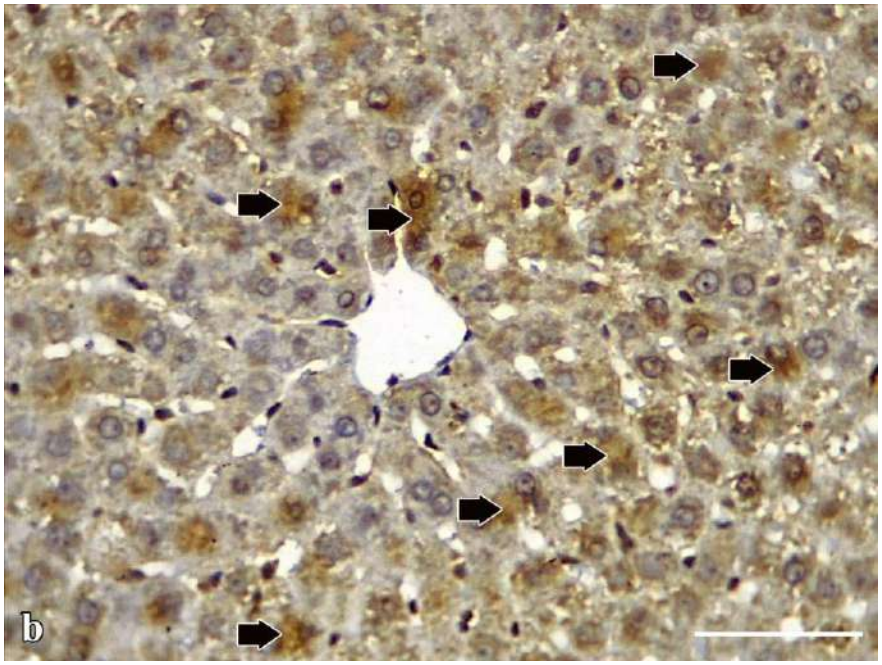

Fig. 5b ZnONPs group showing a strong positive immune reaction for Bax inside the cytoplasm of hepatocytes. Bax × 400, scale bar, 50 μm.

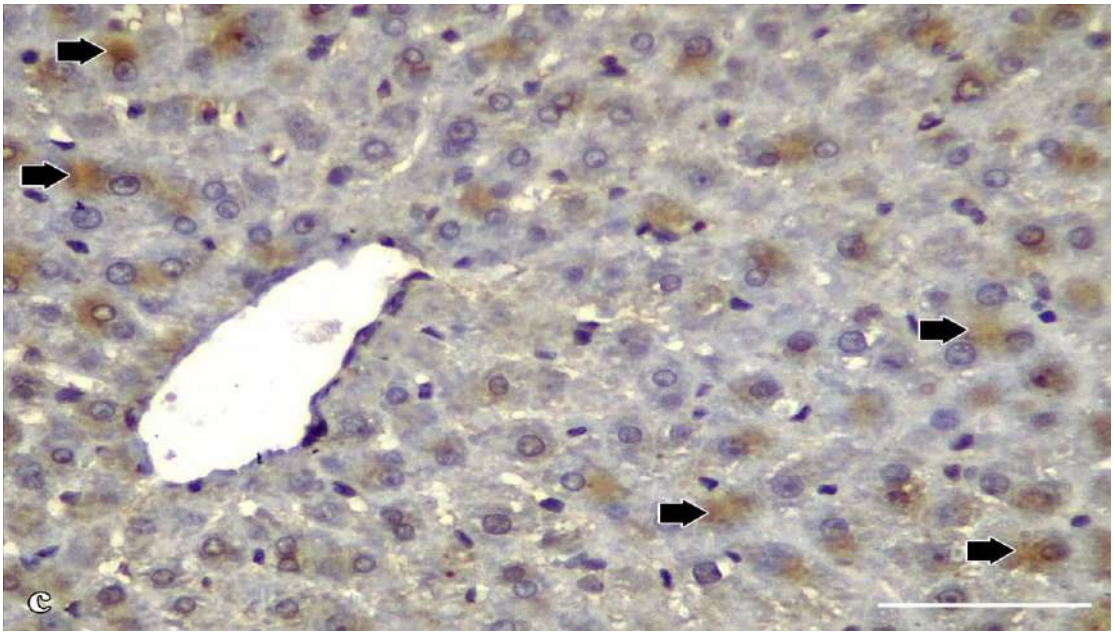

Fig. 5c ZnONPs+ NAR group showing a weak immune reaction for Bax inside the cytoplasm of hepatocytes (arrow). Bax × 400, scale bar, 50 μm.

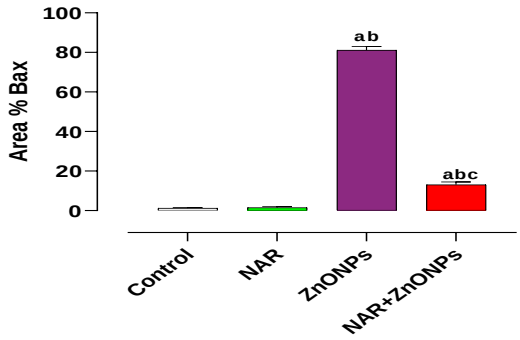

Fig. 5d Effects of NAR on area percent Bax immunoexpression in the rat ZnONPs-induced liver injury model. Data are mean ± standard deviation, *n*= 8. [a] significant vs control group, [b] significant vs NAR group and [c] significant vs ZnONPs group by Welch's ANOVA test followed by Dunnett's T3 test post-hoc multiple comparisons tests, at a *P*-value < 0.05. Abbreviations; NAR, Naringenin; ZnONPs, Zinc oxide nanoparticles.

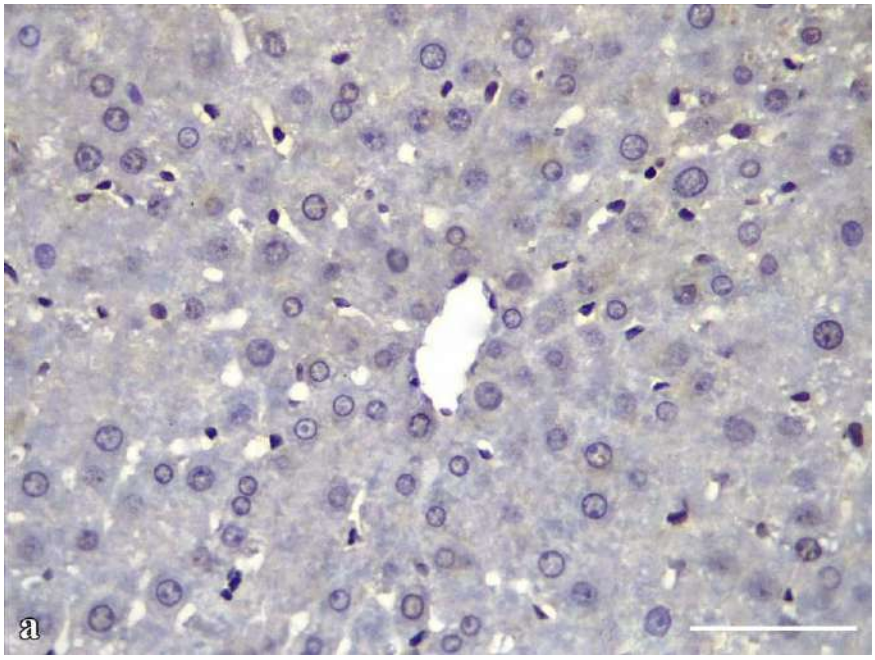

Fig. 6a Control group showing a negative immune group. NF-κB × 400, scale bar, 50 μm.

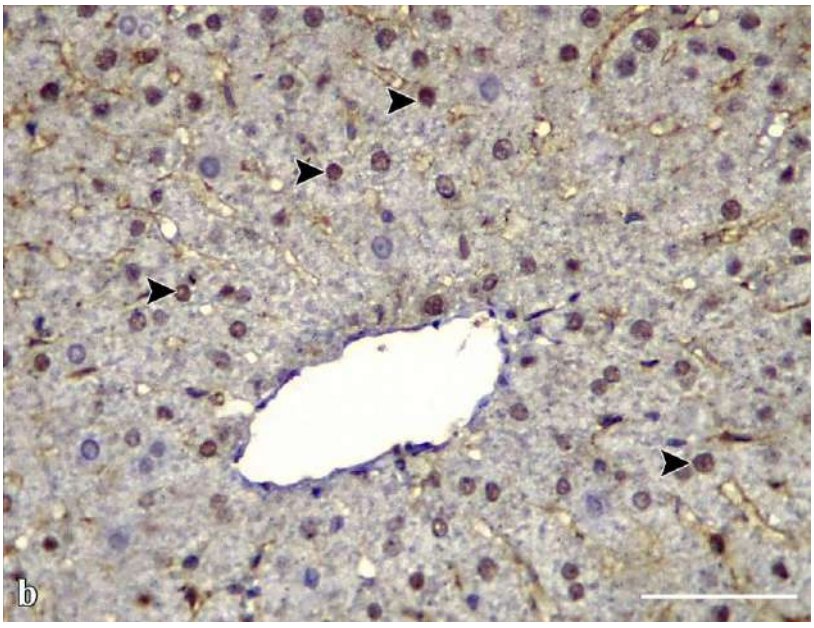

Fig. 6b ZnONPs group showing a strong positive immune reaction for NF-κB of hepatocytes nucleus (arrowhead). NF-κB × 400, scale bar, 50 μm.

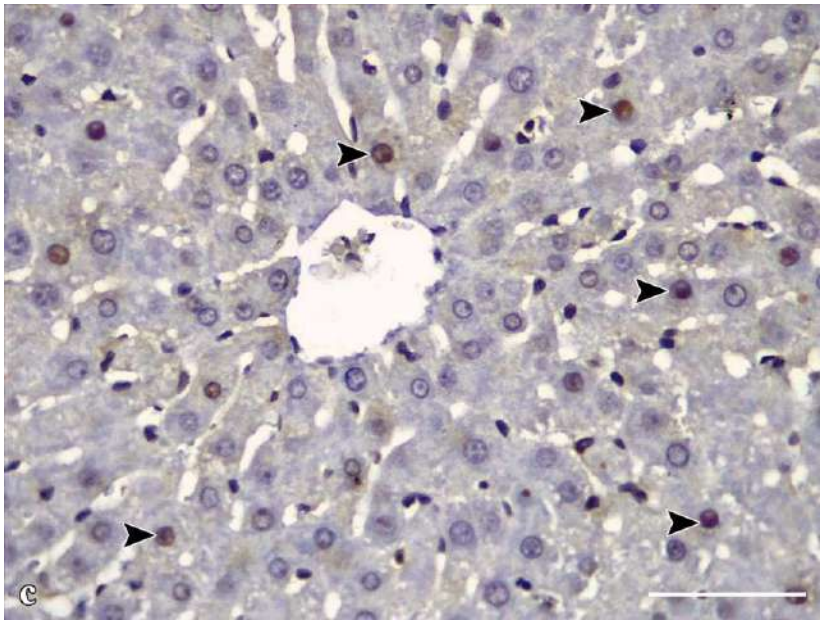

Fig. 6c ZnONPs+NAR group showing a weak positive immune reaction for NF-κB of hepatocytes nucleus (arrowhead). NF-κB × 400, scale bar, 50 μm.

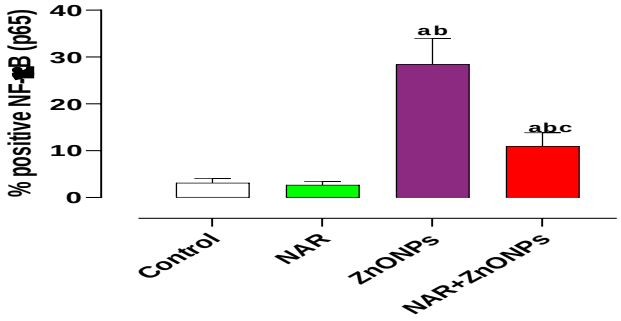

Fig. 6d Effects of NAR on positive nuclear staining of NF-κB (p65) percent in in the rat ZnONPs-induced liver injury model. Data are mean ± standard deviation, *n*= 8. [a] significant vs negative control group, [b] significant vs NAR group and [c] significant vs ZnONPs group by Welch's ANOVA test followed by Dunnett's T3 test post-hoc multiple comparisons tests, at a *P*-value < 0.05. Abbreviations; NAR, Naringenin; ZnONPs, Zinc oxide nanoparticles.

الملخص العربى

النارينحينين يخفف من الإصابة الكبدية في الفئران المعرضة لجزيئات أكسيد الزنك النانوية: التأثير على الإجهاد الالتهابي المؤكسد وموت الخلايا المبرمج

ايمان محمد فاروق [d], علا السيد نافع [b,c*], داليا إبراهيم الوافي [a]

قسم التشريح والاجنة -كلية طب -جامعة الزقازيق - مصر [a]

قسم الشرعى والسموم – كلية الطب -جامعة الزقازيق [b]

قسم الفارما الكلينيكية -كلية صيدلية -جامعه الطائف- المملكة العربية السعودية [c]

قسم الانسجة وبيولوجيا الخلية -كلية الطب-جامعة بنها [d]

أصبح التعرض البشري للجسيمات النانوية أمرًا ثانويًا لا مفر منه لمشاركتهم الهائلة في العديد من التطبيقات الصناعية. تعد الجسيمات النانوية لأكسيد الزنك واحدة من أكثر الجسيمات النانوية لأكسيد المعادن شيوعًا في التطبيقات البيولوجية. مادة النارينجينين هى فلافونويد مشتق من الحمضيات، له خصائص بيولوجية مواتية تعزز صحة الإنسان.

أجريت هذه الدراسة للتحقيق في الدور الدفاعي المحتمل للجسيمات النانوية لأكسيد الزنك مقابل مادة النارجنين الذي تسبب في إصابة الكبد في الفئران من خلال تقييم أنزيمات الكبد، المؤشرات الحيوية الكبدية للإجهاد التأكسدي، عملية الالتهاب ، موت الخلايا المبرمج جنبًا إلى جنب مع الفحص النسيجي لأنسجة الكبد. لذلك، تم تقسيم 32 فأرًا بالغًا بشكل عشوائي إلى أربع مجموعات متساوية مثل مجموعة التحكم، مجموعة المعالجة بالجسيمات النانوية لأكسيد الزنك ومجموعة المعالجة بمادة النارجنينين ومجموعة المشتركة مع مجموعات. تم إعطاء جميع العلاجات لمدة 14 يومًا. أظهرت نتائجنا أن الجسيمات النانوية لأكسيد الزنك تسببت في إصابة الكبد كما هو موثق من خلال الأنشطة المتزايدة الملحوظة للأنزيمات الكبدية ، واضطراب توازن الأكسدة / مضادات الأكسدة الكبدية ، وزيادة التفاعلات الالتهابية الكبدية ، بالإضافة إلى التغيرات المورفولوجية الكبدية الواسعة ، وتراكم ألياف الكولاجين الملحوظ وكذلك الإفراط في التعبير عن موت الخلايا وظهور نووي إيجابي مكثف وملحوظ لعامل موت الخلايا المبرمج في الانسجة مع مجموعة الجسيمات النانوية لأكسيد الزنك بينما انخفض بشكل كبير أنشطة إنزيمات الكبد ، واستعاد توازن الأكسدة / مضادات الأكسدة ، والالتهاب المعكوس ، وتسبب في تراكم أقل لألياف الكولاجين وموت الخلايا المبرمج بوساطة مادة النارجنين.

لقد خلصنا الى ان مادة النارجنين مادة مكملة الجسيمات النانوية لأكسيد الزنك حيث يحسن من وظيفة الكبد وهيكله من خلال إمكاناته المضادة للأكسدة والمضادة للالتهابات